Embryonic lineage analysis using three-dimensional, time-lapse in-vivo fluorescent microscopy

Minden, Jonathan, Kam, Zvi, Agard, David, Sedat, John, Alberts, Bruce

Jonathan Minden, Zvi Kam, David A. Agard, John W. Sedat, Bruce Alberts, "Embryonic lineage analysis using three-dimensional, time-lapse in-vivo fluorescent microscopy," Proc. SPIE 1205, Bioimaging and Two-Dimensional Spectroscopy, (1 August 1990); doi: 10.1117/12.17781

SPIE.

Event: OE/LASE '90, 1990, Los Angeles, CA, United States

Embryonic lineage analysis using three-dimensional, time lapse in vivo fluorescent microscopy

Jonathan Minden, Zvi Kam[1], David Agard[2], John Sedat[2], and Bruce Alberts

University of California, San Francisco, Department of Biochemistry and Biophysics,
and [2]Howard Hughes Medical Institute Structural Biology Unit,
San Francisco, California 94143
[1]Weizmann Institute of Science, Polymers Department, Rohovot, Israel 76100

ABSTRACT

Drosophila melanogaster has become one of the most extensively studied organisms because of its amenability to genetic analysis. Unfortunately, the biochemistry and cell biology of *Drosophila* has lagged behind. To this end we have been microinjecting fluorescently labelled proteins into the living embryo and observing the behavior of these proteins to determine their role in the cell cycle and development. Imaging of these fluorescent probes is an extremely important element to this form of analysis. We have taken advantage of the sensitivity and well behaved characteristics of the charge coupled device (CCD) camera in conjunction with digital image enhancement schemes to produce highly accurate images of these fluorescent probes in vivo. One of our major goals is to produce a detailed map of cell fate so that we can understand how fate is determined and maintained. In order produce such a detailed map, protocols for following the movements and mitotic behavior of a large number of cells in three dimensions over relatively long periods of time were developed. We will present our results using fluorescently labelled histone proteins as a marker for nuclear location[1]. In addition, we will also present our initial results using a photoactivatable analog of fluorescein to mark single cells so that their long range fate can be unambiguously determined.

1. INTRODUCTION

Drosophila embryonic development can be divided into two distinct phases of growth. The first phase is characterized by 13 rounds of rapid nuclear division as a syncytail mass where there are no cell membranes separating individual nuclei. The syncytial mitotic cycles are lacking any detectable G1 or G2 phase and only very low levels of RNA transcription can be detected. It appears that the main purpose of this stage of development is to increase the number of nuclei as quickly as possible. Genetic analysis has revealed that a number of genes required for specification of the segmented body plan are active during this syncytial period. Therefore, it is believed that the overall coordinate system which defines the anterior-posterior and dorsal-ventral axes is established during this period. The syncytial mitoses occur as synchronous waves emanating from the ends of the oval shaped embryo. The end of the syncytial phase is brought about by the formation of cells membranes around each nucleus. A variety of studies involving either genetic or physical manipulation of the embryo indicate that just at the end of cellularization every cell in the embryo is fated for a particular function. The cellular mitotic cycles exhibit defined G1 and G2 periods with high levels of RNA synthesis. The newly formed cells enter mitosis not in a synchronous pattern but as spatially and temporally defined groups or domains of cells.[2] There are 25 bilaterally symmetric mitotic domains where all the cells within a domain behave similarly with respect to the time of mitosis and the orientation of the mitotic spindle. Some domains are composed of a large number of cells while others are made up of single cells in a metamerically repeated pattern. We were interested to understand how a cell decides to reside in a particular mitotic domain. Is the decision based on cell lineage or on positional cues? In addition we wished to determine the long range fate of cells within a mitotic domain. Are the cells in a particular mitotic domain restricted to a limited set of fates and are the cells in neighboring mitotic domains restricted to different sets of fate? In order to address these sorts of questions, techniques were developed to 1) globally label nuclei with a vital marker, 2) record nuclear

position as a function of time in three dimensions, and 3) mark single cells for long term (greater than 12 h) observation.

Global marking of nuclei was accomplished by microinjecting flourescently labelled histone proteins into syncytial stage *Drosophila* embryos. The histones diffused throughout the cytoplasm and were incorporated into chromatin during periods of DNA replication. Imaging of nuclei was done with an inverted microscope equipt with a scientific grade, Peltier cooled charge coupled device (CCD). Focus, fluorescent filter selection, and image acquisition was controlled by a stand-alone computer workstation. Using fluorescently labelled histones, we followed the movement of a large number of nuclei from the tenth syncytial nuclear cycle, through cellularization, to the first cellular division at the end of cycle fourteen. Two types of developmental maps were generated; one displayed the lineage relationship of all the cells at the end of the syncytial phase and the other charted the fate of these cells with respect to mitotic domain residency. Superposition of these two maps indicate the the decision to reside in a mitotic domain is governed by position in the embryo and not on cell lineage.

In order to follow the fate of cells within a particular mitotic domain to determine their presice tissue fate, syncytial stage embryos were microinjected with a photoactivatable form of fluorescein[3] (referred to as caged fluorescein or C'2AF) covalently linked to superoxide dismutase (SOD). The C'2AF-SOD diffused throughout the cytoplasm and was present in every cell after cellularization. The caged fluorescein dye within individual cells was activated using a UV microbeam to un-cage the fluorescein molecule. This procedure yielded embryos that had only a limited number fluorescently marker cells with very little background fluorescence. Early experiments on single cell lineage tracing indicates that this technique will be extremely fruitful.

2. MATERIALS AND METHODS

2.1. Preparation of fluorescently-labelled proteins

A detailed protocol for labelling histone proteins will be published elsewhere (J. Minden, manuscript in preparation). Briefly, purified histones were bound to double stranded DNA cellulose under conditions that permit nucleosome formation[4]. The purpose of this step was to ensure that only the exposed surface of the proteins were modified during a thirty minute, room temperature incubation with N-hydroxy-succinimide tetramethyl rhodamine (NHSR) (Molecular Probes, Oregon) in a buffer containing 0.2M NaCl, 20 mM potassium HEPES, pH 7.4, and 1 mM Na_3EDTA. After the unreacted fluorochrome was removed by repeated washing of the resin, the NHSR-labelled nucleosome/DNA cellulose resin was packed into a small column and the histone proteins were eluted with a 0.2 to 2M NaCl gradient containing 20 mM Tris-HCl, pH 7.4 and 1 mM Na_3EDTA. The fractions that contained histones H2A and H2B, determined by polyacrylamide gel electrophoresis, were pooled and concentrated by centrifugation in a spin dialysis apparatus (Centricon, 10,000 dalton cutoff). Small aliquots were frozen in liquid nitrogen and stored at -80°C. The stored NHSR-histones prepared and stored in this fashion were stable for more than one year.

Superoxide dismutase (Sigma, St. Louis MO) at 6 mg/ml in 0.1 M $NaHCO_3$ pH 9.2 was labelled with a 60 mg/ml solution of di-(2-nitro 5-carboxymethyl benzyl) carboxyfluorescein N-hydroxy succinimidyl ester (C'2AF, a gift of Dr. T. Mitchison, UC San Francisco) in dimethyl sulfoxide at a ratio of .45 mg C'2AF/ 1 mg SOD. The reaction was incubated at room temperature for 30 min. All procedures were performed at room temperature under a safe light to prevent premature activation of the fluorescein. The sample was then applied to a Sephadex G-100 column and eluted with 0.1 M $NaHCO_3$, pH 9.2 buffer. The protein fractions were pooled and concentrated with a change of buffer to 15 mM KPO_4, 150 mM NaCl pH 7.4 by centrifugation in a spin dialysis apparatus (Centricon, 10,000 dalton cutoff). The C'2AF-SOD at a concentration of 10 mg/ml was stored a 4°C in a light tight container.

2.2. Microinjection of the labelled proteins

Wild-type Oregon R embryos were collected at ten minute intervals on small petri dishes that contain standard egg laying media (Roberts, 1986). The embryos were hand dechorionated and mounted on a 20X50 mm cloverslip through the use of a thin strip of glue prepared by dissolving the adhesive from double-sided Scotch-brand tape in heptane. The embryos were dried slightly over $CaCl_2$ for 8-12 min and then overlayed with a drop of halocarbon oil (Halocarbon Products, series 700, Hackensack NJ). Injections of a 0.4 mg/ml solution of NHSR-histone H2A/2B protein or of a 10 mg/ml solution of C'2AF-SOD were made at 50% egg length using a Lietz micromanipulator. Injection needles (3 μm diameter) were pulled from 1.2mm OD x 0.9mm ID glass capillary tubes (FHC, omega dot type, Brunswick ME). The time from collection to injection was less than thirty minutes, so that the labelled protein could diffuse evenly throughout the embryo cytoplasm, prior to cycle 10 and produce uniformly-labelled blastoderm nuclei.

2.3. Recording the movements of the chromatin labelled with NHSR-histone

The NHSR-histone injected embryos were observed on an Olympus inverted microscope equipped for epifluorescence, using a 40X,1.3 N.A. oil immersion objective lens (Olympus) and a high performance rhodamine filter set (Omega Optical, Brattleboro VT). The embryo was illuminated with a 100W mercury arc lamp attenuated 20-fold with a 520 +/-10 nm band pass filter (Omega Optical, Brattleboro VT). The images were acquired by a Peltier-cooled CCD camera (Photometrics Ltd., Tuscon AR) equipped with a 1340 X1037 pixel CCD chip (Kodak-Videk). The entire process of focusing the objective, opening and closing shutters, and storing the digital data was controlled by a Microvax II workstation (Digital Equipment Corporation) coupled to a 32 M-byte Mercury Zip 3232+ array processor (Mercury Computer systems Inc., Lowell MA) and a Parallax model 1280 display system (Parallax Graphics Inc., Santa Clara CA). The data was stored on a large format, 2 G-byte, optical disk (Emulex Corp./Optimem 1000, Costa Mesa CA)). A typical recording was made in two parts; the first segment captured the syncytial divisions as a series of single focal plane exposures of 0.1 sec taken every 23 sec, while the second segment began at cellular blastoderm and recorded the cycle 14 mitoses as a repeating series of similar exposures taken at eight consecutive focal planes spaced 2.5 μm apart (the focal series was repeated every 23 sec). Only the top six focal planes were used to generate the three-dimensional movies, because the two deepest sections contained unincorporated or degraded NHSR-histone that blurred the images. The embryos were kept until hatching to ensure that the neither the injection of histones nor the illumination during the recording session had damaged the embryo.

2.4 Photactivation and recording the movement of single cells past cycle 14

A different arrangement of embryos was used for single cell lineage analysis. In order to peer more deeply into the embryo (the embryo is 200 μm in diameter), we positioned the embryos on a thin, transparent, oxygen permient teflon membrane (YSI Inc., Yellow Springs OH) which was stretched over a specially machined carrier. The embryos were dried and covered with halocarbon oil. The embryos were mounted on the microscope so that the objective was immersed in the halocarbon oil. The teflon membrane support was necessary to prevent the embryos for becoming anoxic during the recording period. Photoactivation was performed on a Ziess standard microscope using a Ziess 63X oil objective with a correction collar. The correction collar was carefully adjusted to match the refractive index of the halocarbon oil. A 200 μm pinhole was mounted at the field diaphragm in the epifluorescence tube of the microscope. An electronic shutter was placed between the mercury lamp and the pinhole in the epifluorescence port. The C'2AF-SOD was activated with a 10 s pulse of 365 nm light using a standard DAPI fluorescence filter set (Ziess). Generally we activated cells during mitosis at which point they roundup and swell to twice their interphase size. This can be easily seen by normal Kohler illumination. Typically we viewed the mitotic behavior on a television monitor connected to a Nuvicon video camera (COHU Corp. San Diego CA) which was mount on a trinocular head. Once activated, the embryos are transferred to the CCD inverted microscope system and observed with a 25X Ziess water/glycerol/oil objective with the correction collar adjusted to match the refractive index of the halocarbon oil. Typically a

recording is composed of a series of 10 x 10 μm optical sections recorded every 5 min for 12 h. One of the complications of using fluorescein as a fluorescent dye in vivo is that the embryo has broad band autofluorescence in the same wavelength region as fluorescein, thus contributing a substantial background. Two steps were taken to alleviate this problem. First, a narrow band fluorescence excitation filter was used to limit excitation of the endogenous fluorochromes. Second, since the autofluorescence signal is excited over a broad range, a second image using a rhodamine filter set was taken as a background image. The fluorescein activated cells did not contribute to the rhodamine signal. Thus when the two images were scaled appropriately and subtracted, the resultant clearly showed only the photoactivated cells.

2.5. Data manipulation and computer programming.

The bulk of the data processing and computer model building were performed on a Vax 8650 computer system (Digital Equipment Corp.) with attached Parallax display stations. All of the software used is also compatible with the Microvax II system. In order to obtain high quality stereo projections of the three-dimensional data stacks, the images were computationally manipulated to enhance the local contrast around each pixel [5]. Each set of optical sections was then converted into a three-dimensional array of pixel intensities, rotated in space, and projected onto an imaginary image plane to produce a pair of stereo images [6].

The tracings shown were generated interactively with the computer graphics display system, by entering selected data with an on-screen cursor. The modelling software package, written in Fortran, allows the viewing of simultaneously-updated stereo images in a time-lapse fashion [7]. The images shown here were photographed using a Dunn digital camera system (Log E-Dunn) with Technical Pan 2415 film.

An automated scheme for tracing nuclear movements was developed to aid in the analysis of lineage tracing experiments. The images were first scanned in order to detect all contiguous areas or patches of fluorescence signal. This was done by a procedure of ordering all pixel intensities and scanning for neighboring bright elements. Threshold levels were set so that the patches would not grow too large, thus keeping neighboring nuclei distinct. Not all of the objects identified by this scheme were nuclei and additional logical parameters were applied to distinguish between nuclei and aberrant structures in the images. This procedure was carried out for two dimensional images as well as three dimensional data sets. The resultant of the nuclear identification program was a file of the coordinate positions of each nucleus in an image. These files were analyzed to determine the linages of individual nuclei and their descendents by identifying the location of the nucleus in the first image of a recorded series and then finding the nearest neighbor in each subsequent image. The positional data files were also used to produce idealized views of the embryo during development. The nuclei were displayed as solid spheres, similar to molecular modelling routines. These cartoon images allow one to appreciate the three dimensional movements of the cells without the need for stereo projections (data not shown).

3. RESULTS AND DISCUSSION

3.1. Tracing nuclear behavior from cycle 11 to the completion of cycle 14

The 5000 cells that form the the cellular blastoderm in cycle 14 can be subdivided into at least 25 mitotic domains that seem to reflect the result of spatially patterned cell determination processes [2, 8]. In order to test for a possible role of cell lineage in these cell determination events, we have followed the detailed behavior of the nuclei in an area of the embryo that contains several intersecting mitotic domains. The field of view is shown as an unshaded area in Figure 1; it encompasses a lateral region anterior to the cephalic furrow that will form six mitotic domains . This region contains more than forty nuclei at nuclear cycle 11; in three hours, at 23°C, it developed from nuclear cycle 11 through the end of cycle 14 (4 nuclear divisions), producing more than three hundred cells that can be grouped into mitotic domains according to the time and pattern of the cell division that ends their 14th nuclear cycle. Most of the data presented here

were generated from a single embryo that went on to generate a normal larva after the recording was terminated.

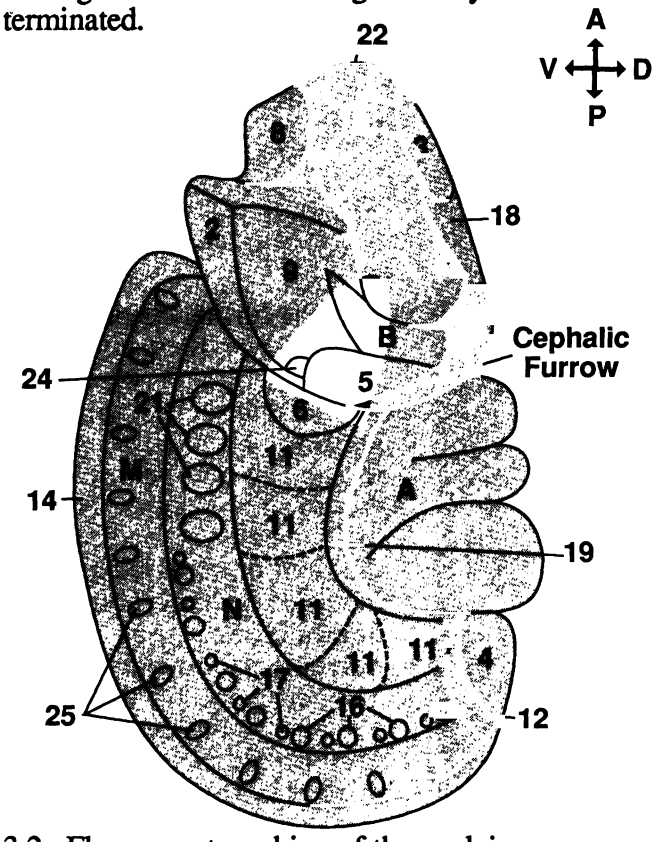

Figure 1. Lateral View of Cycle 14 Mitotic Domains. Detailed map of cycle 14 mitotic domains from Foe (1989). Unless stated otherwise, the embryo is oriented with the anterior end up and the ventral side on the left in all figures. The mitotic domains are assigned numbers to indicate the temporal sequence of domain mitoses, with letters to indicate groups of cells that either not divide (A and B) or divide asynchronously (M and N). The unshaded area designates the field of view utilized in this work. Because we have focused on the domains anterior to the cephalic furrow, domain 6 was omitted from further analysis.

3.2. Fluorescent marking of the nuclei

Syncytial nuclei were visualized by microinjecting fluorescently-labelled calf-thymus histones, which became incorporated into chromatin during subsequent periods of DNA replication. In order to ensure that the fluorescent histones were distributed evenly throughout the syncytial cytoplasm, injections were performed within thirty minutes of egg deposition (prior to nuclear cycle 5). Our previous studies demonstrated that these calf-thymus histones do not interfere with normal development in unirradiated embryos (Minden and Alberts, in preparation). Although prolonged irradiation of fluorescent-histone injected embryos with intense light is lethal, by exposing the embryo to brief pulses of attenuated light we can observe these nuclei for many hours without detectable damage to the embryo.

3.3 Following the descendents of single nuclei from cycle 11 to cellular blastoderm

A series of images of a living embryo taken at 0.375 min intervals that allow individual cycle 11 nuclei and their progeny to be traced through three syncytial divisions is presented in Figure 2. The progeny of a single nucleus are marked to demonstrate the type of nuclear movements seen in the embryo. Each of the three vertical columns starts at metaphase of a nuclear cycle (cycles 11, 12, or 13 respectively) and continues through interphase and prophase of the following nuclear cycle. (A cycle is defined as beginning at interphase and ending at telophase). Since the syncytial nuclei remain in the cortex of the embryo throughout this period, recordings can be made with a fixed focal plane.

3.4. Analysis of nuclear behavior prior to gastrulation using computer based tools

After marking the location of the nucleus in every frame with an interactive cursor, a computer software package for two- or three-dimensional image analysis [7] was used to digitize, store, and organize

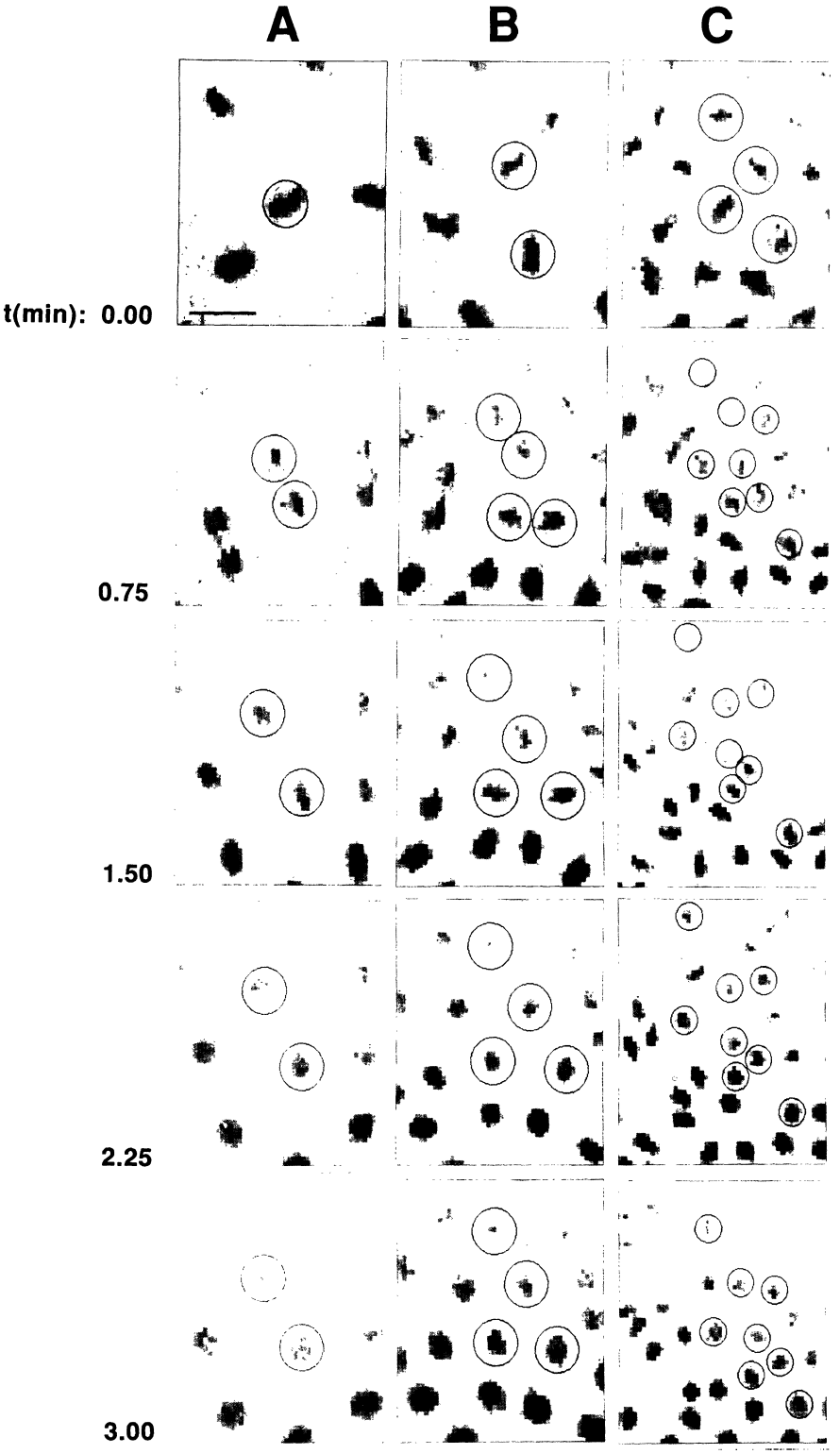

Figure 2. Fluorescent Images of Nuclei from Metaphase of Nuclear Cycle 11 to Interphase of Nuclear Cycle 14.
A wild-type Oregon R embryo was hand dechorionated, mounted on its side on a coverslip, desiccated, and covered with halocarbon oil to prevent further drying. The embryo was then injected at 50% egg length with a 0.4 mg/ml solution of fluorescent histone H2A/H2B. The images were recorded as described in Results. A series of images of a small area of the field of view taken at the indicated intervals is shown to demonstrate the nuclear movements during mitosis. The progeny of the single nucleus in the center of the first image in panel A are marked with a black square. The temperature during the recording period was 23.8°C. As defined, each nuclear cycle starts with interphase and ends with the following telophase (see Foe and Alberts, 1983).
(A) Metaphase of nuclear cycle 11 to interphase of nuclear cycle 12.
(B) Metaphase of nuclear cycle 12 to interphase of nuclear cycle 13.
(C) Metaphase of nuclear cycle 13 to interphase of nuclear cycle 14.
Bar = 10 mm.

all of the nuclear positions. Figure 3 presents a display of the movements and divisions of the marked nuclei in Figure 2. Because of the complexity of the movements, the data is presented as a stereo pair, in which the elapsed time is translated into depth. Except for the anaphase movements, all movements of neighboring nuclei are coordinated; so that the monolayer of nuclei tends to

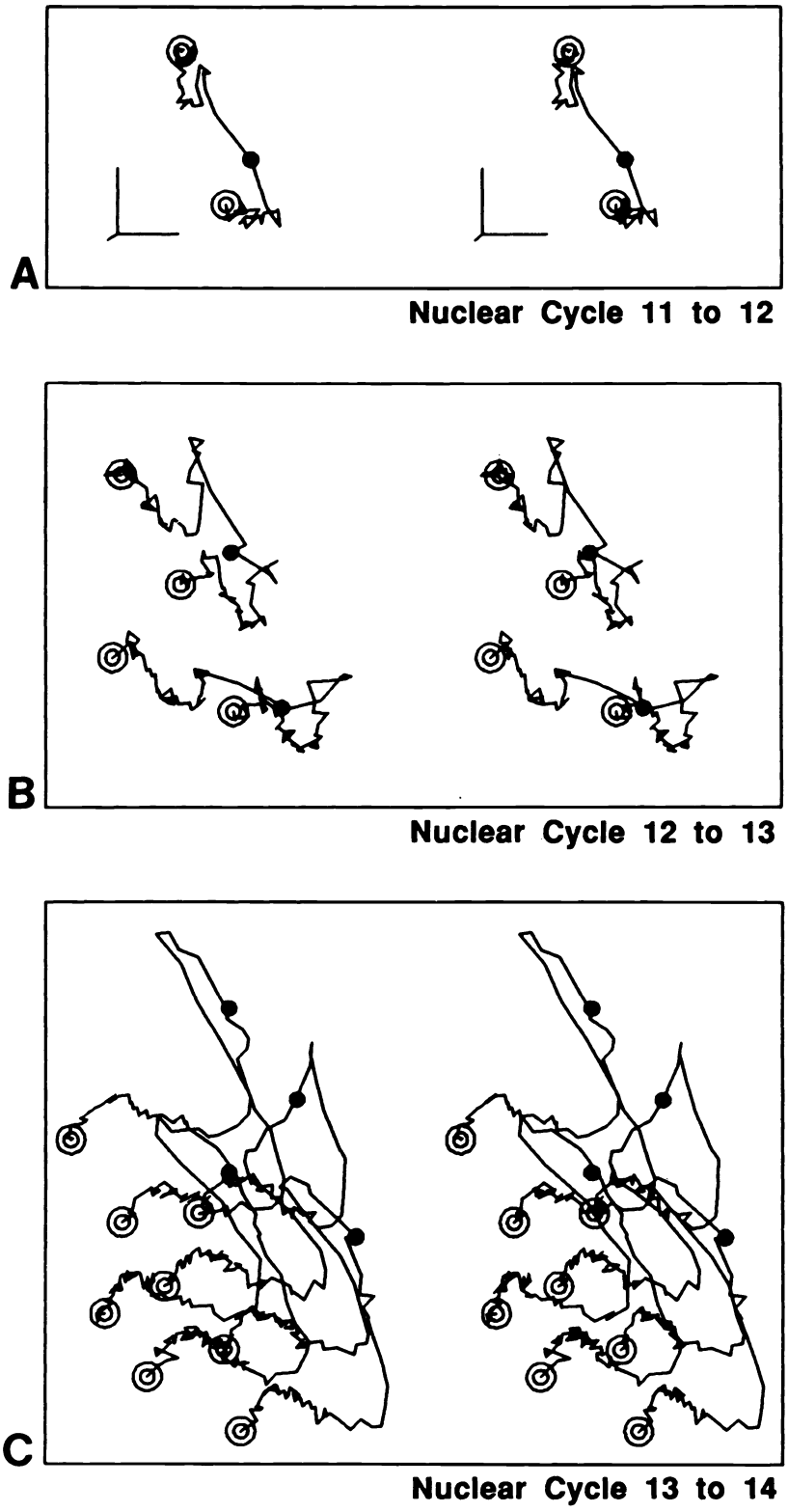

Figure 3. Computer Generated Representations of Tracing the Movements of Nuclei from Metaphase of Nuclear Cycle 11 to Interphase of Nuclear Cycle 14.
The movements of the nuclei shown in Figure 2 were traced at 23 sec intervals and are projected here as stereo images, where each trace shows the path taken by sister nuclei as they separate from each other starting at metaphase in one cycle (closed circles) and continuing to metaphase in the subsequent cycle (concentric open circles). In this representation, the depth component increases linearly with increasing time with a straight line connecting successive positions separated by 23 sec intervals. In order to obtain an uncluttered perspective of the nuclear movements, the models were rotated 20 degrees about both the horizontal and vertical axes (as shown by the axes in Panel A). Time increases as the nuclei move away from the viewer if the stereo pairs are viewed with the aid of stereo glasses, while the opposite perspective is seen with unaided "cross-eyed" viewing. The tilt angle between left and right images is 6 degrees.
(A) Metaphase of nuclear cycle 11 to metaphase of nuclear cycle 12.
(B) Metaphase of nuclear cycle 12 to metaphase of nuclear cycle 13.
(C) Metaphase of nuclear cycle 13 to the start of cellularization in cycle 14.

move as a unit. However, whereas the nuclei maintain an evenly spaced configuration during cycles 11 and 12, the nuclei in nuclear cycle 13 come very close to each other at the end of anaphase and form small, short lived clusters of three to five nuclei (see Figure 2C, t=1.50 min). In an attempt to identify any

patterning of these syncytial divisions three conclusion were drawn. First, there was no correlation between the angle of division of mother nuclei and daughters or between daughter nuclei. Each nuclear cycle had a characteristic pattern of movement and wave of mitosis that was consistent from one embryo to the next. Third, the only movement pattern that was suggestive of any global arrangement was the anaphase movement during nuclear cycles 12 and 13. During these periods the nuclei performed a dance that showed mirror symmetry around the lateral midline of the embryo (Figure 4). We are testing dorsal-ventral mutant embryos to see whether this phenomenon is an early indicator of dorsal-ventral polarity.

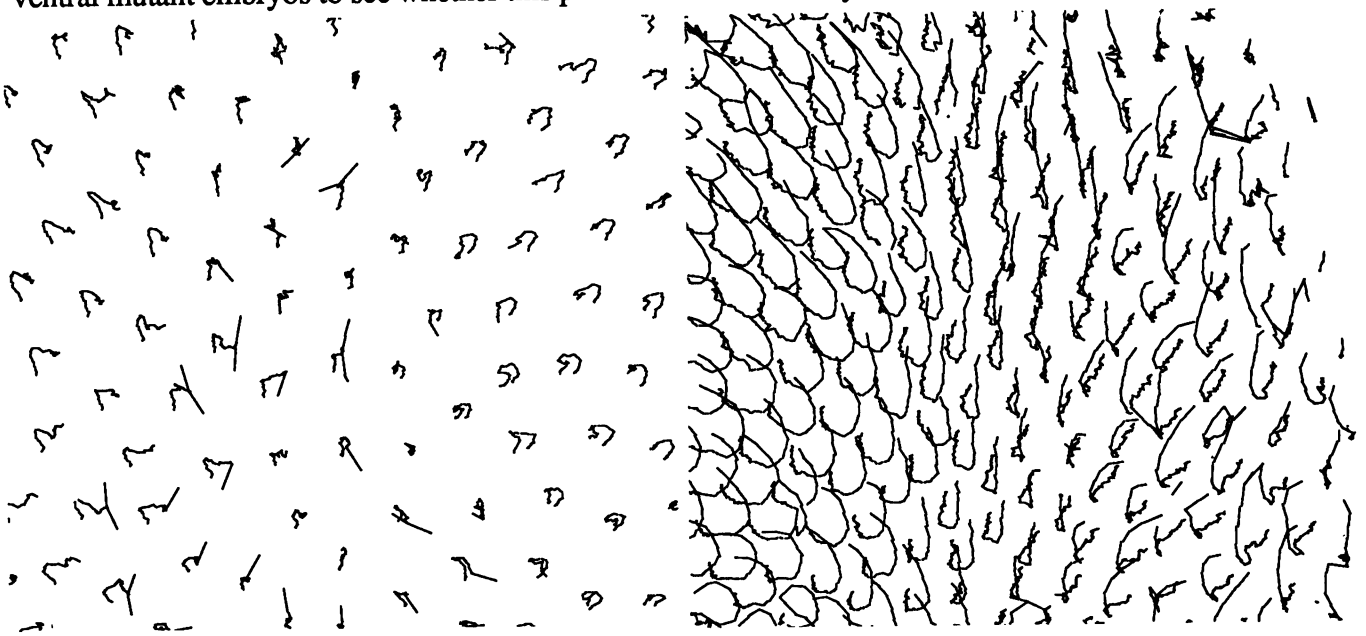

Figure 4. Automatic Analysis of Anaphase Movements in Nuclear Cycles12 and 13. The left panel shows cycle 12 and the right panel shows cycle 13. Each plot represents a subset of the entire field centered around the lateral midline. Notice the mirror symmetry of the movements around the lateral midline. Also notice that the pattern of nuclear movement was different in the two nuclear cycles shown.

3.5. Lineage map for a patch of 40 cycle 11 nuclei

In order to produce a lineage map of the entire field of view shown in Figure 1, the type of analysis presented in Figure 3 for a single cycle 11 nucleus and its progeny was extended to include all of the nuclei in the field. Single nuclei were never found to be isolated from their siblings by being completely surrounded by unrelated nuclei; this clustering means that there is no nuclear mixing between nuclear cycle 11 and 14; the nuclei do not change their neighbors during this period. Every aspect of the mitoses that occur in the syncytial blastoderm stage embryo appears to be disordered, except for the cycle 12 and 13 anaphase movements (data not shown).

3.6. Assigning each of the cycle 14 cells to their respective mitotic domains

The field of view examined in Figure 1 covers portions of seven mitotic domains that are designated as domains 1, 2, 5, 6, 9, 24 and B (Figure 1). These domain numbers have been assigned according to the temporal order of the entry of their nuclei into mitosis of cycle 14; the exception is domain B in which the cells fail to divide during the first three hours of gastrulation [2]. The cells within each mitotic domain also have a characteristic orientation of their mitoses; thus, the cells in domains 1, 2, 5, and 24 divide parallel to the surface of the embryo, while the cells in domain 9 divide perpendicular to this surface (Foe, 1989). In order to assign each cell to a particular mitotic domain, we needed to extendour recordings past the cellular blastoderm stage so as to be able to observe the time and orientation of its fourteenth division.

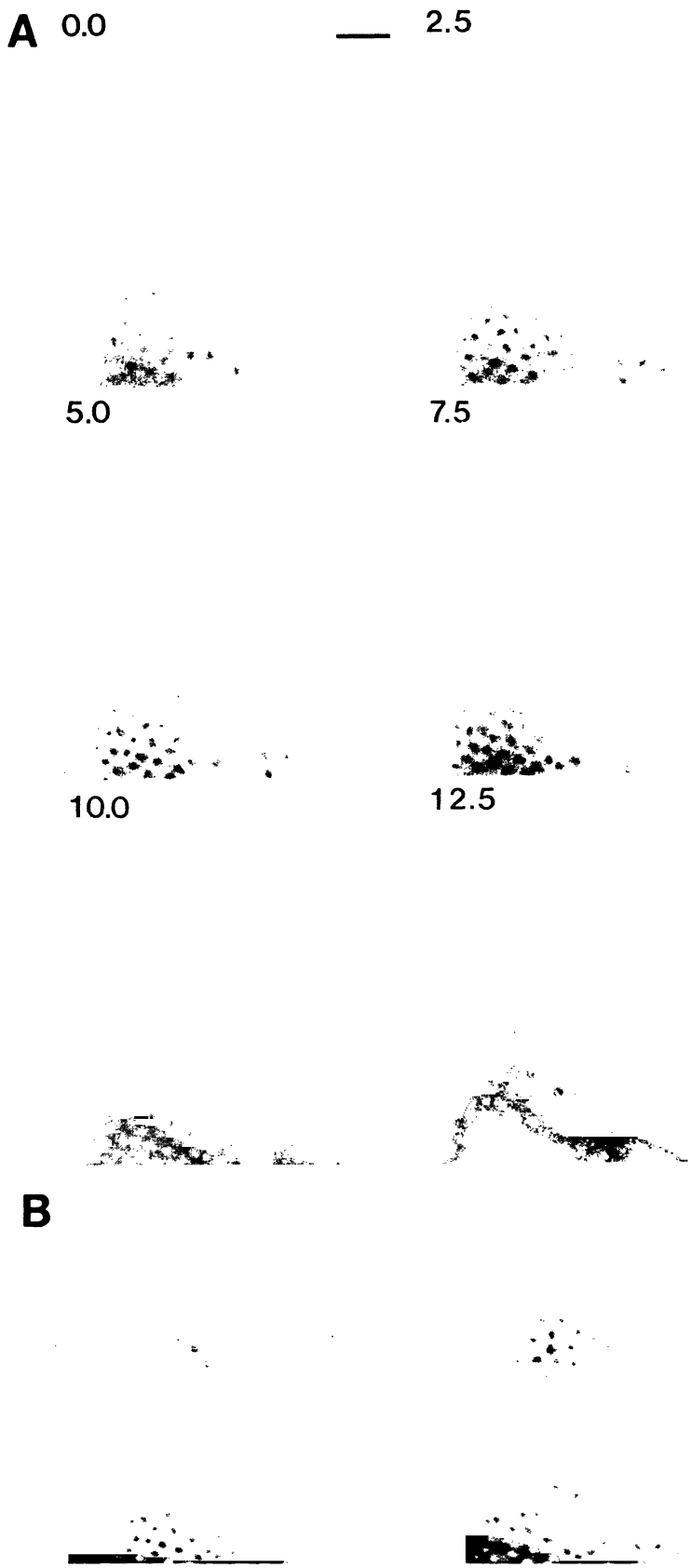

Figure 5. Obtaining Three-dimensional Fluorescent Images of the Nuclei in a Gastrulation Stage Embryo.
(A) Six un-enhanced photographs of CCD-images taken in rapid succession, the first photograph shows the top-most focal plane; subsequent photographs proceed towards the center of the embryo at 2.5 mm intervals. The time interval between the recording of each photograph (an optical section) was approximately 3 s, this frequency is sufficient to generate three-dimensional images without blurring due to nuclear movement. This data was digitally stored and computationally enhanced and rotated in space, +/-15 degrees, to produce the pair of stereo images in Panel B.
(B) Stereo pair of the data set shown in Panel A. The anaphase nuclei in domain 1 (for domain identification, see Figure 7A) appear less fluorescent, this is probably because of the depletion of the fluorescent-histone pool at the time of cellularization. In domain 5 several of the nuclei are in metaphase.
Bar = 20 mm.

The task of following a cell throughout cycle 14 without losing sight of it for a short period proved to be difficult. As soon as cellularization was complete, gastrulation was initiated, and many of the cells moved out of any single focal plane. In order to trace the fate of all these cells simultaneously, it became necessary to view the nuclei in the living embryo in three-dimensions. This was done by recording the image from a precisely-spaced series of focal planes taken at regular time intervals (Figure 5A), and computationally manipulating the data to generate a pair of stereo images. This process was repeated every 23 sec to produce a time-lapse movie of the cell movements during gastrulation. A typical stereo pair of the gastrulating embryo taken from the time-lapse recording is shown in Figure 5B; the cephalic furrow can be seen in this micrograph as a horizontal line. Some of the cells in domain 1 have just completed mitosis (located in the upper-right portion of the image, also see Figure 7A for domain identification); their nuclei are smaller, more densely packed, and slightly less fluorescent. Some cells in domain 5 are in metaphase and their chromosomes are condensed to form an elongated, box-like structure (located just below and to the right of the center of the image). Because the cells that form the cephalic furrow move so deeply into the interior of the embryo, it was not possible to follow them continuously with our data set.

3.7. Determining domain boundaries in the gastrulation stage embryo

In order to determine the boundaries between all of the mitotic domains in the field of view, a map indicating both the orientation and the temporal sequence of the mitoses that end cycle 14 was generated (Figure 6). In this map the orientation of division is indicated by the shape of the symbol, where circles represent cells that divide parallel to the surface of the embryo, triangles indicate cells that divide perpendicular to the surface, squares indicate cells that did not divide in the period of the recording, and diamonds indicate cells that were lost from view in the cephalic furrow. For those cells that remained visible, the time of mitosis is indicated by a clock-face; the earliest divisions are indicated by the open clock-face, while the latest divisions are indicated by the filled clock-face. The first mitotic events after cellularization occur 82 min into cycle 14 in mitotic domain 1 (for domain identification, see Figure 8A); the mitosis of cells in domain 5 begins a few minutes later and after another eleven minutes, the cells in domain 9 begin to divide. The cells that constitute domain 24 divide almost 50 minutes after the first divisions in domain one.

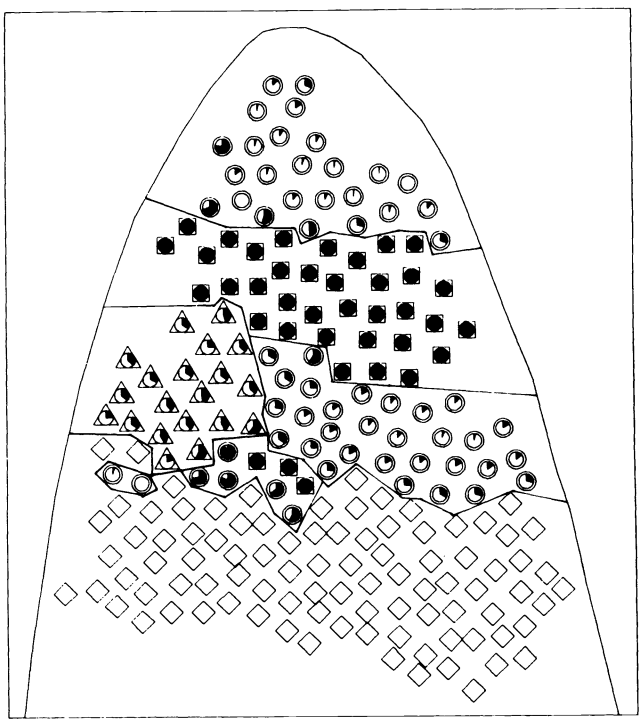

Figure 6. Identification of Cycle 14 Mitotic Domains.
This map shows the orientation and the time that the nuclei of the cycle 14 embryo enter mitosis, indexed on the position of the nuclei at the start of cellularization. Circles indicate cells that divide in the plane of the embryo, triangles indicate cells that divide perpendicular to the surface of the embryo, squares indicate cells that did not divide in the period of the recording, and diamonds indicate cells that were lost from view in the cephalic furrow. The clock-face in the center of all cells that remained visible indicates the time of division, where the open clock-face represents the earliest divisions, which occurred after 82 min of cycle 14, a half-filled clock-face represents cells that divided after 106 min of cycle 14, and the closed clock-face represents the end point of the recording 130 min after the start of cycle 14. The identifiable mitotic domains are separated by solid lines (compare with Fig. 1).

The variation in the temporal sequence of mitoses within a mototic domain demonstrates that the mitotic domains do not divide synchronously, but contain temporal waves of mitoses. In domains 1 and 9 these waves appear to originate from two or more separate centers. It is not clear whether this is an indication of a finer organization of the mitotic regions.

3.8. Correlation of the lineage map with the domain fate map

What might one expect to observe, using the approach described here, if the lineage of a cell was important in determining a mitotic domain? If the decision to form a particular mitotic domain is made prior to cycle 11, the sets of eight lineage-related cells in Figure 4D should never cross the border between two domains. If the decision to form a mitotic domain is made during interphase of cycle 11, four of the eight related cells in a group should be on one side of a domain boundary and four should be on the other side. If the decision to form a mitotic domain is instead made during cycle 12, cells should cross a domain border as pairs. Finally, if the decision to form a mitotic domain is made during cycle 13, the same pattern of single cells spanning a domain border should be observed in different embryos. On the other hand, if the decision to form a mitotic domain is entirely delayed until cycle 14, there should be no relationship between cell lineage and mitotic domains in the embryo.

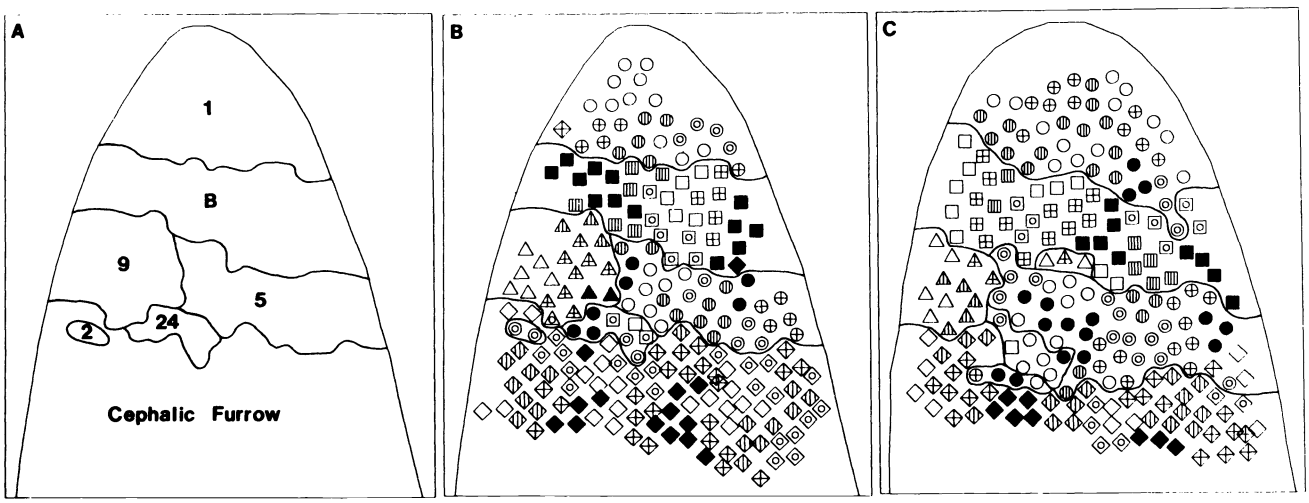

Figure 7. Fate Map of the Blastoderm Embryo.
Each cell in the cellular blastoderm stage embryo was followed from the start of cellularization until it either divided or until the end of our recording 130 min after the start of cycle 14. The fate of each cell is indicated by a different shape, where circles indicate parallel divisions, triangles indicate perpendicular divisions, squares indicate cells that did not divide, and diamonds indicate cells that were lost from view in the cephalic furrow (as is Figure 6). The fate symbols are positioned according to the location of the nucleus at the start of cellularization. The fate symbols are also marked with respect to their lineage history according to the markings in Figure 4 and thus represent a superposition of the lineage and fate maps.
(A) Mitotic domains assigned according to the time and orientation of cell division.
(B) Superposition of the lineage and the domain fate maps This hybrid map reveals that a single lineage-related group of eight cells (seen as clusters of cells with similar internal patterns) can have several fates. One particular group, the group with vertically striped symbols in the left-central portion of the map, had three cells in domain 9, two cells in domain 5, and two cells in domain B.
(C) Superposition of the lineage and fate maps for a second embryo. This map confirms the results in B. It also demonstrates the random nature of lineage partitioning with respect to domain boundaries, since the two embryos do not correspond with respect to lineage patterns or the organization of lineages across domain borders. The only common feature is the position and shape of the mitotic domains. The differences in the size of the mitotic domains can be explained by the fact that the second embryo was rotated slightly so that the lateral midline appears shifted to the left.

The lineage and the domain fate maps are superimposed in Figure 7. The data for a single embryo (Figure 7B) show no obvious correlation between cell lineage and residency in a particular mitotic domain. For example, there are many instances of odd numbers of cells on opposite sides of a boundary between two domains and there are several cases where groups of eight cells have many different fates. These results indicate that the decision to behave one way or the other is not made until at least cycle 13.

If a series of lineage-dependent choices that are more complex than those described above dictate the behavior of the cells (e.g. if some decisions made earlier than others), one would expect some features of the lineage and fate maps to be maintained from embryo to embryo. A map comparing lineage and cell fate was therefore constructed for a second embryo. The results, shown in Figure 7C, show no correlation with Figure 7B in terms of the relationship between lineage and domain boundaries. The only similarity is in the overall position and shape of the mitotic patches. The lack of correspondence from embryo to embryo indicates that the domain boundaries are not drawn until cycle 14. We conclude that the decision of a cell to reside in a particular mitotic domain is probably based entirely on positional cues, with no role for cell ancestry.

3.9. Initial experiments on long range lineage analysis in living embryos

It is clear that cell lineage has no role in determining which cells reside in each mitotic domain. It remains to be determined if the mitotic domains play a role in fixing the fate of the cells within a domain. Are all the cells in a particular mitotic domain fixed in their fate and can neighboring domain cells ever adopt the same fate? In order to address these questions one must follow individual cells or groups of cells from the time they demonstrate their domain residency to the end of their developmental course when they contribute to the formation of a specific larval structure. Single cells were marked by injecting embryos with a photoactivatable fluorescein analog bound to superoxide dismutase. The caged fluorescein has no fluorescent properties until the caging groups are removed upon exposure to 365 nm light. Since fluorescein is a small molecule and can diffuse through cell membranes and gap junctions, the caged fluorescein was covalently linked to SOD. This protein was chosen as the carrier for the caged fluorescein because of its long half-life in cells as a completely soluble cytoplasmic protein. In addition, SOD acts to scavenge oxide radicals that are produced during fluorescent activation of the fluorescein. Another unexpected benefit of using SOD is that it appears to be transported out of the yolk into the cells, thus increasing the amount of caged dye in the cells. Single cells were activated for fluorescence by imaging a pinhole on the embryo. Once activated the embryos were observed for more than 12h without any lose of viability. Figure shows the progress of a singley marked cell over time. Since these are preliminary experiments we have not determined precisely what the fates of these cells are. By carefully examining the developmental course of individual cells from specific mitotic domains we will be able to generate a complete and detailed map the Drosophila development to the same resolution as has been done for C. Elegans. This developmental map would then act as a guide for studying a large variety of developmental mutants to determine more precisely the genetic defect and molecular mechanism of the processes that contribute to the formation of a complex multicellular organism.

Figure 8. Time series of photoactivated cells in vivo. A single cell on the ventral midline of an embryo that was injected with C'2AF-SOD during the syncytial stage of growth was activated with a 10 s pulse of 365 nm light. There are four groups of four optical sections. The top most optical section is in the top left corner of each time set. Each image represents a separation of 10 μm into the embryo. The four time points are 4, 8 , 12, and 16 h after fertilization. In the first focal series a single cell is seen near the surface of the embryo. 4 h later one can detect two cells where one cell is still at the surface and the other is 10 μm deeper in the embryo. By 8 h the number of cells has increased and are found more anterior and 30 μm from the surface. At the end of the recording, when the embryo was on the verge of hatching as a larvae, the cells spread out in a line along the anterior-posterior axis and are distributed between 30 - 40 μm below the ventral surface of the embryo. This data set demonstrates that the injected and photoactivated embryos survive and that it is now possible to follow the fate of a small number of cells of long periods of time.

4. ACKNOWLEDGMENTS

This work was supported in part by NIH grants GM31286-06 to B.M.A., GM25101-09 and GM32803-03 to J.W.S., and GM31627 to D.A.A. and by the Howard Hughes Medical Institute (D.A.A. and J.W.S.). D.A.A. was also supported by a grant from the NSF Presidential Young Investigator Program. J.S.M. was supported by a fellowship from the Helen Hay Whitney Foundation and Lucille P. Markey Foundation. We would like to thank Hans Chen, Yasushi Hiraoka, Andy Belmont, Michael Paddy, and Mary Rykowski for help in software development and Bill Sullivan, Kathy Miller, Doug Kellogg, Chris Field, and Bill Theurkauf for helpful discussions. We would especially like to thank Dr. Victoria Foe for sharing her data with us prior to publication.

5. REFERENCES

1. Minden, J. S., Agard, D. A., Sedat, J. W., and Alberts, B. M. (1989). Direct cell lineage analysis in Drosophila melanogaster by time-lapse, three- dimensional optical microscopy of living embryos. J. Cell Biol. *109*, 505-516.
2. Foe, V. E. (1988). Mitotic domains reveal early commitment of cells in Drosophila embryo. Development *107*, 1-22.
3. Mitchison, T. J. (1989). Polewards microtubule flux in the mitotic spindle: evidence from photoactivation of fluorescence. J. Cell Biol. *109*, 637-652.
4. Palter, K. B. and Alberts, B. M. (1979). The use of DNA-cellulose for analyzing histone-DNA interactions. J. Biol. Chem. *254*, 11160-11169.
5. Belmont, A. S., Sedat, J. W., and Agard, D. A. (1987). A three-dimensional approach to mitotic chromosome structure: evidence for a complex hierarchical organization. J. Cell Biol. *105*, 77-92.
6. Agard, D. A., Hiraoka, Y., Shaw, P., and Sedat, J. W. (1988). Fluorescent microscopy in three dimensions. Methods in Cell Biol. *30*, 353-377.
7. Chen, H., Sedat, J. W., and Agard, D. A. (1989). Manipulation, display, and analysis of tree-dimensional biological images. In Handbook of confocal microscopy, J. Pawley, ed. (Electron Microscopy Society of Am.), pp. 127-136.
8. Foe, V. E. and Odell, G. M. (1989). Mitotic domains partition fly embryos, reflecting and early cell biological consequences of determination in progress. Am. Zool. *29*, 617-652.